Received 19 February 2019; revised 15 March 2019; accepted 27 March 2019. Date of publication 4 April 2019;
date of current version 26 April 2019. The review of this paper was arranged by Editor C.-M. Zetterling.

Digital Object Identifier 10.1109/JEDS.2019.2908419

On the Ammonia Sensing Performance and Transmission Approach of a Platinum/Nickel Oxide/GaN-Based Metal-Oxide-Semiconductor Diode

I-PING LIU[1], CHING-HONG CHANG[2], YEN-MING HUANG[2], AND KUN-WEI LIN[3]

1 Department of Chemical Engineering, National Cheng Kung University, Tainan 70101, Taiwan
2 Advanced Optoelectronic Technology Center, Department of Electrical Engineering, Institute of Microelectronics, National Cheng Kung University, Tainan 70101, Taiwan
3 Department of Computer Science and Information Engineering, Chaoyang University of Technology, Taichung City 41349, Taiwan

CORRESPONDING AUTHOR: K.-W. LIN (e-mail: kwlin@cyut.edu.tw)

This work was supported in part by the Chaoyang University of Technology (CYUT) and Higher Education Sprout Project, Ministry of Education, Taiwan, through the Project "The Research and Development and the Cultivation of Talent for Health-Enhancement Products."

ABSTRACT New platinum (Pt)/nickel oxide (NiO)/GaN-based metal-oxide-semiconductor (MOS) diode-type ammonia sensor was fabricated and studied. In addition, a new grey polynomial differential recovery (GPDR) model was developed for the application of data transmission. The studied Pt/NiO/GaN-based MOS diode shows good ammonia sensing performance at relatively high temperatures ($\geq$423 K). A very high sensing response of 244.2 under 1000 ppm NH_3/air gas and a low detecting level of 2 ppm NH_3/air are obtained at 423 K. The studied device also shows operating flexibility in the applied forward and reverse voltages, and good reversibility in ammonia sensing. In order to expand the practical application of ammonia sensing, a GPDR model was developed to effectively reduce *data redundancy* by 64.22% and achieve a recovery rate of 99.79% compared with the original data. Therefore, the studied sensor device provides promise for ammonia sensing applications.

INDEX TERMS Ammonia, Pt/NiO/GaN, operating flexibility, Schottky diode, GPDR.

I. INTRODUCTION

Ammonia (NH_3) is a compound of nitrogen and hydrogen, and an important raw material for various downstream nitrogen-based products. Ammonia is widely applied in chemical, food, and semiconductor industries, and in agriculture, fertilizer, factories, refrigeration systems, medical treatment, and living environments [1]–[5]. Based on the widespread applications indicated above, globally produced ammonia is on a linearly increasing trend with 140 million tons in 2015 [6], [7]. Yet, higher-concentrations of ammonia can lead to severe irritation of the respiratory tract, skin, eyes, mouth, nose, throat, and other moist mucous membranes [8]. Under the international standards for the toxicity level of ammonia for humans, the short-term exposure over 15 min needs to be limited to 25-35 ppm and the Time-Weighted-Average (TWA) over an 8 h period should not exceed 25 ppm [9], [10]. The concentration that is immediately dangerous to life or health (IDLH) is 300 ppm [11]. So, the development and fabrication of high-performance ammonia gas sensors to reliably and continuously monitor and detect the ammonia leakage are indispensable for human and environmental safety.

Over recent decades, numerous n-type semiconducting metal-oxides (SMOs), e.g., TiO_2, SnO_2, ZnO, WO_3, and ITO, have been reported to produce resistor-type ammonia sensors with good performance [2], [12]–[15]. In addition, a p-type SMO material, i.e., nickel oxide (NiO), has also been reported to fabricate smart resistor-type ammonia sensors due to its inherent advantages, including a wide energy bandgap, high melting point, and chemical stability [16], [17]. On the other hand, metal-semiconductor (MS) Schottky diodes

based on III-N materials, e.g., ZnO/AlGaN/GaN and platinum (Pt)/AlGaN/GaN, have been reported for ammonia sensing applications [18]–[20]. The AlGaN/GaN heterostructures with high-density, two-dimensional electron gas (2DEG) arising from the piezoelectric and spontaneous polarization effects are sensitive to changes in atmospheric conditions [20]–[22].

As IoT technology becomes ever more mature, the trend is to analyze and monitor gas conditions by transmitting the data of various sensors scattered over a large space to the server/cloud computer. However, the large amount of sensing data being transmitting through the network will cause network transmission congestion and rapid power consumption of the sensors. Therefore, it is important to reduce redundant data transmission and restore the transmitted data [23]–[25].

The grey system theory was proposed by Prof. Ju-Long in 1982 [26]. It has been widely used in economics, meteorology, hydraulics, transportation, environmental protection, etc. It is a non-statistical theory that can use less data to make prediction models and correlations. In the grey system, GM(1, 1) is most commonly used and processed in the first-order differential accumulation generation method, which is inconsistent with the characteristics of the transient response of the gas sensor. Hsieh *et al.* proposed a grey polynomial method to solve the problem with the image [27]. However, the characteristics of the sensed data cannot be clearly presented by using the grey polynomial method. Based on this algorithm, we developed a new grey polynomial difference model (GPDM) to achieve a reduction in the amount of transmitted data [28]. However, there are two drawbacks need to be improved. One is that the error rate is still exist between the measured sensing data and the reduced redundancy data. The other is that the reduction data has not been further recovered to the original data. Hence, we also developed a new gray polynomial difference recovery (GPDR) model to overcome the above problems.

In this work, a new approach based on the combination of a Pt catalytic metal, a NiO oxide layer, and GaN/AlGaN heterostructures was used to fabricate a metal-oxide-semiconductor (MOS) diode-type ammonia sensor. Experimentally, good ammonia sensing properties, including a very high sensing response of 244.2 under introduced 1000 ppm NH_3/air gas and a lower detecting level 2 ppm NH_3/air at 423 K, were obtained. In addition, operating flexibility in both the applied forward and reverse voltages and good reversibility in ammonia sensing were acquired. Furthermore, a new Grey polynomial difference recovery (GPDR) model was proposed to effectively reduce data redundancy; a comparison to the original measured data was made. Data can be recovered with an accuracy rate of 99.79% using this GPDR model.

II. EXPERIMENTS PROCEDURE

The epitaxial structure used in the studied sensor device was grown on a silicon substrate using a metal organic chemical vapor deposition (MOCVD) system. This structure included a buffer layer, a 1.5 μm-thick GaN layer, a 22 nm-thick $Al_{0.2}Ga_{0.8}N$ layer, and a 20 nm-thick GaN cap layer. The as-grown samples were first treated using an inductively-coupled-plasma reactive ion etching (ICP-RIE) system to achieve mesa isolation. Thereafter, acetone, hydrogen chloride (HCl), and deionized water were used to clean the sample surfaces. Ohmic contacts were formed by sequentially depositing Ti/Al/Ti/Au metals with thicknesses of 10 nm/100 nm/10 nm/100 nm on the top surfaces of the GaN cap layer, using vacuum thermal evaporating and alloying with a rapid thermal annealing (RTA) system at 900°C in N_2 ambience for 90 s. A 15 nm thick NiO layer was deposited using a radio-frequency (RF) sputtering process with a power of 50 W, a working pressure of 3 mtorr, and a 10 sccm Ar ambience. After the RF sputtering process, the samples were annealed using RTA at 400°C in an N_2 ambience for 30 min. Finally, Schottky contacts were formed by evaporating a 20 nm-thick Pt metal with an effective area of 2.05×10^{-3} cm^2. A schematic cross-sectional diagram of the studied sensor device is depicted in Fig. 1. The experimental current-voltage (I-V) characteristics and transient response curves were measured with a Keithley 4200 semiconductor parameter analyzer.

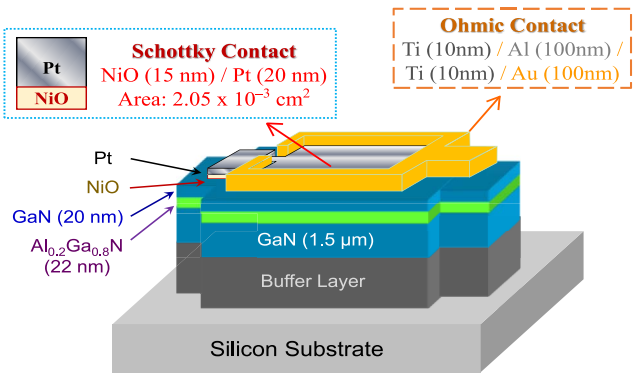

FIGURE 1. Schematic cross section diagram of the studied device.

III. GREY POLYNOMIAL DIFFERENTIAL AND RECOVERY MODEL (GPDR)

In order to construct the ammonia gas sensing model, a new grey polynomial differential and recovery algorithm (GPDR) was developed. First, an ammonia gas transient response model was developed based on the GPDM [28]. Second, the differences between the original results (ammonia gas transient response) and GPDM data were determined. Third, these error simulation data were replaced with the actual sensing data. Fourth, three fixed points were added between every 100 points. This approach has two advantages: One is to instantly detect if the sensor is still alive, and the other is to avoid simulation and experimental errors when restoring data. The final GPDR model simulated curve preserves the features of the original curve. Compared with the original data, 64.22% of the data can be reduced before transmission,

and 99.79% of the data can be recovered by GPDR after transmission.

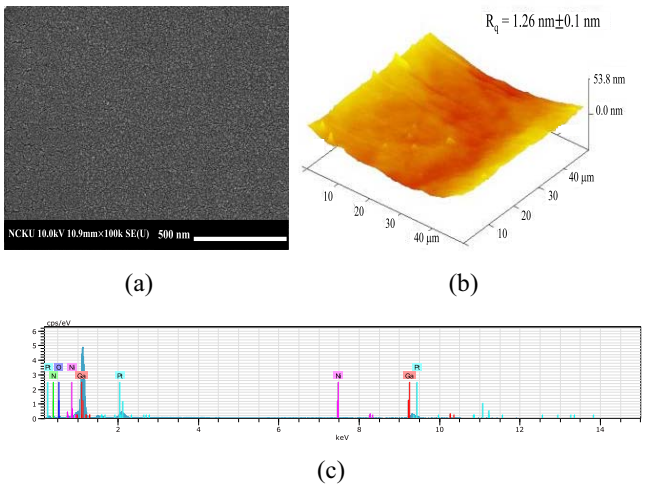

(a) (b)

(c)

El	AN	Series	unn. C [wt. %]	norm. C [wt. %]	Atom. C [at. %]	Error [wt.%]
Ga	31	K	51.87	69.49	48.67	2.34
N	7	K	7.47	10.01	34.90	2.05
O	8	K	2.91	3.90	11.90	0.90
Pt	46	L	11.92	15.97	4.00	0.56
Ni	28	K	0.47	0.64	0.53	0.09
Total:			74.64	100.00	100.00	

FIGURE 2. (a) Top-view scanning electron microscopy (SEM), (b) atomic force microscopy (AFM), and (c) energy dispersive spectrometer (EDS) analyses of the studied Pt/NiO/GaN-based sensor device.

IV. RESULTS AND DISCUSSION

The top-view scanning electron microscopy (SEM) images of the studied Pt/NiO/GaN-based device are shown in Fig. 2(a). Clearly, uniform and smooth surface morphology is evident. The related atomic force microscopy (AFM) images are shown in Fig. 2(b). The corresponding root-mean-square (RMS) roughness is 1.26±0.1 nm. The energy dispersive spectrometer (EDS) element analysis of the studied device is provided in Fig. 2(c). Unn. C and norm. C are the unnormalized and the normalized concentration in weight percentage of the element, respectively. Atom. C is the atomic weight percentage and Error is the error in the weight percentage. Peaks in the Pt, Ni, O, Ga, and N are observed. The EDS analysis demonstrates that no other impure element was found in the studied device.

The measured I-V characteristics, under different concentrations of ammonia gas at 423 K and 473 K are shown in Figs. 3(a) and (b), respectively. Apparently, the current increases with the increased ammonia concentration under

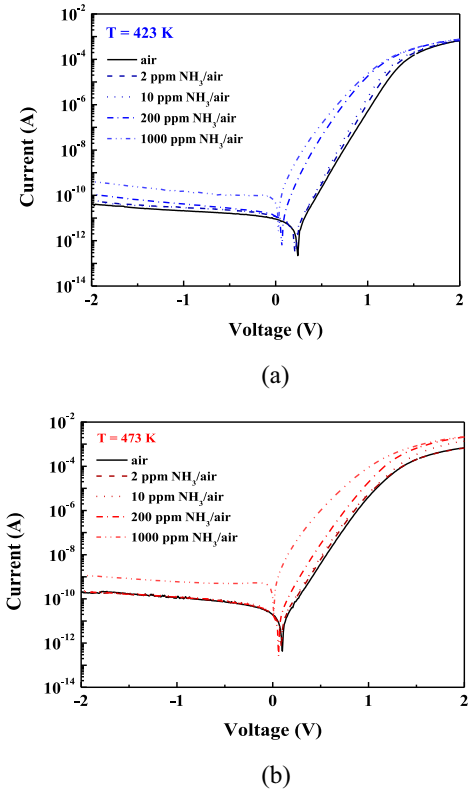

FIGURE 3. Current-voltage (I-V) characteristics of the studied device, under different concentrations of ammonia gas, at (a) 423 K and (b) 473 K.

applied forward and reverse voltages. In addition, the current variation (ammonia sensing performance) is sensitive to the operating temperature. For the studied device, due to the lower dissociation efficiency of ammonia molecules, the ammonia sensing behavior (current variation) is negligible when the temperature is lower than 423 K [19], [20]. Therefore, the studied device should be operated under relatively higher temperatures (> 423 K) for ammonia sensing. As previously reported, the ammonia sensing mechanism of Schottky diode-type sensors can be interpreted as follows [19]. Under the used catalytic Pt metal, ammonia molecules are adsorbed on the Pt metal surface and dissociated into nitrogen and hydrogen atoms [19]. Some of these hydrogen atoms that diffuse through the Pt bulk reach the Pt/NiO interface. These accumulated hydrogen atoms are polarized by the total internal electric field ε_i of NiO and GaN to achieve a dipole layer at the interface [29]. The presence of this dipole layer causes an electrical field ε_d which is in the contrary direction toward ε_i. The formation of ε_d leads to reduced magnitude of ε_i, energy barrier in NiO, and an effective Schottky barrier height from $q\phi_b$ to $q\phi_b'$, as shown in Fig. 4 [30]. Thus, based on the reduction of the Schottky barrier height, the conducting current is increased when the ammonia gas is introduced.

The ammonia sensing response S_R, as a function of temperature of the studied device under the applied forward voltage of $V_{appl} = 0.4$ V and the reverse voltage of

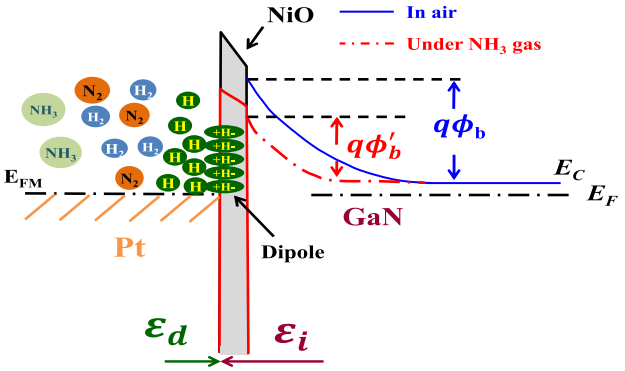

FIGURE 4. Representative energy band diagrams of the studied device under introduced ammonia gas.

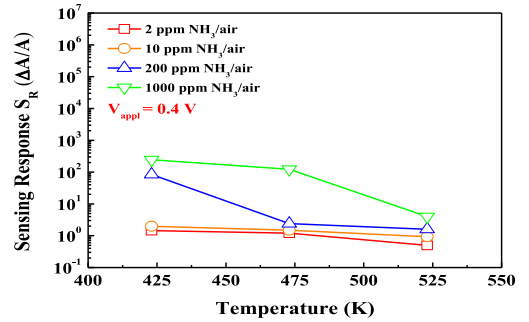

(a)

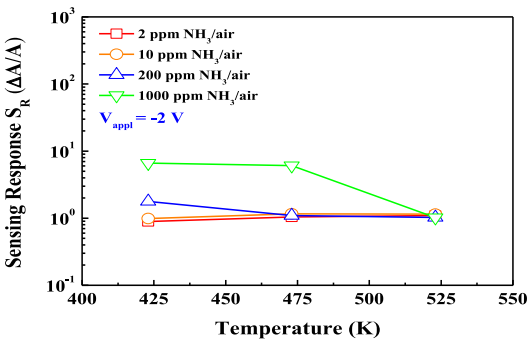

(b)

FIGURE 5. Ammonia sensing response S_R as a function of temperature of the studied device under applied (a) forward voltage of $V_{appl} = 0.4$ V and (b) reverse voltage of $V_{appl} = -2$ V.

$V_{appl} = -2$ V, is shown in Figs. 5(a) and (b), respectively. The sensing response S_R is defined as [19], [20]:

$$S_R = \frac{I_{NH_3} - I_{air}}{I_{air}}, \tag{1}$$

where I_{NH_3} and I_{air} are currents measured in ammonia-containing ambience and air, respectively. The S_R is increased (decreased) with the increase (increase) in ammonia concentration (temperature), as shown in Fig. 5. For instance, under the forward voltage of $V_{appl} = 0.4$ V, S_R is increased from 1.4 to 244.2 when the ammonia concentration is increased from 2 ppm to 1000 ppm NH_3/air at 423 K, as shown in Fig. 5(a). The significant S_R value of 244.2 is superior to that of reported Schottky diode-type ammonia sensors [18]–[20]. Moreover, under 1000 ppm NH_3/air gas, the S_R drastically decreases from 244.2 to 2.5 as the temperature increases from 423 K to 523 K. The studied Pt/NiO/GaN-based MOS diode exhibits ammonia sensing ability even under an applied reverse voltage, as shown in Fig. 5(b). Under the applied voltage of $V_{appl} = -2$ V, the S_R increases from 0.9 to 7.3 once the ammonia concentration increases from 2 ppm to 1000 ppm NH_3/air at 423 K. Therefore, the studied device shows ammonia sensing capability and operating flexibility under applied voltages both forward and reverse.

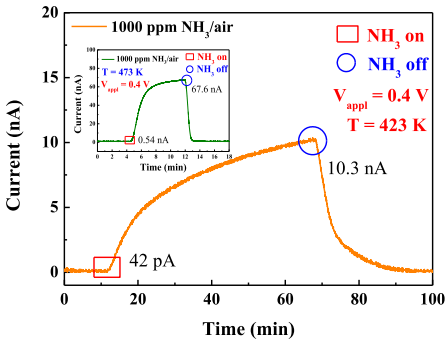

FIGURE 6. Transient response of the studied device upon exposure to 1000 ppm NH_3/air gas at 423K. The corresponding performance at 473 K is shown in the inset.

The transient response of the studied device upon exposure to 1000 ppm NH_3/air gas at 423 K is shown in Fig. 6. The inset shows the corresponding performance at 473 K. The applied forward voltage is kept at $V_{appl} = 0.4$ V. Clearly, the conducting current is rapidly increased (decreased) upon the introduction (removal) of ammonia gas. The sensing speed is obviously enhanced with the increase in temperature, as illustrated in Fig. 6. Also, the recovery action (removal of NH_3 gas) is faster than the response action (introduction of NH_3 gas). In order to evaluate the sensing speed, the response (recovery) time constant is defined as the time required to achieve 90% of the full response (recovery) action [31]–[33]. Under 1000 ppm NH_3/air gas, the studied device has a relatively longer τ_a of 41.5 min at 423 K. This value can be drastically decreased to 1.2 min at the higher temperature of 523 K. Yet, the corresponding τ_b value is decreased from 12.6 min to 0.15 min when the temperature is increased from 423 K to 523 K. Hence, the recovery action of the studied device is faster than the response one, as indicated above. This may be caused by the relatively complicated steps and processes of the dissociation of NH_3 and H_2 molecules on the Pt surface. Therefore, a longer τ_a is needed to complete the full response action.

Figure 7 shows three repetitive dynamic responses of the studied device under 1000 ppm NH_3/air gas at 473 K. The corresponding performance at 523 K is shown

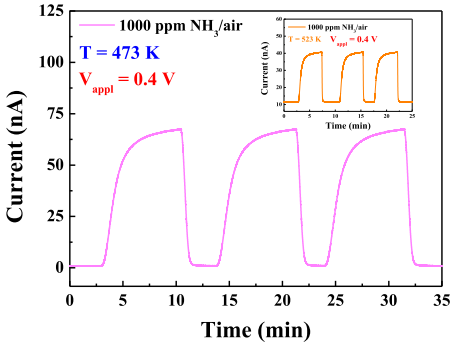

FIGURE 7. **Three repetitive dynamic responses of the studied device under 1000 ppm NH_3/air gas at 473 K. The corresponding performance at 523 K is shown in the inset.**

in the inset. The applied forward voltage is fixed at V_{appl} = 0.4 V. Clearly, the studied device shows reversible current variations upon the exposure and removal of ammonia gas; therefore, the studied Pt/NiO/GaN MOS device shows good repeatability and reversibility for ammonia sensing applications.

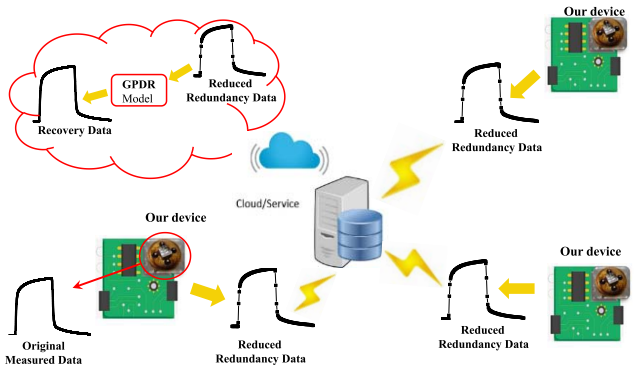

FIGURE 8. **A schematic diagram of sensing transmission of the studied device for IoT application.**

Figure 8 illustrates a schematic diagram of sensing transmission of our studied device for IoT application. First, ammonia gas is sensed by our studied ammonia sensor (original sensing data), and then the data is transmitted to the server through the reduced redundancy operation. Finally, the transmission data is recovered by using the proposed GPDR algorithm. During the sensing transmission process, it is necessary not only to reduce the amount of data transmitted, but more importantly, to increase the ratio of recovery. Practically, under introduced ammonia gas, the amount of data at the initial stage is not large. So it is a good choice to predict or simulate the sensing curve with the grey system algorithm. GM(1, 1) is most commonly used as a predictive approach in grey systems [34]. Figure 9 shows the corresponding simulated results from GM(1, 1). In order to obtain the ammonia sensing data (original) and sample data (simulated) for comparison, the mean relative recovery error rate (MRE) is defined as [35]:

$$\mathrm{MRE}(\%) = \frac{1}{n}\sum \frac{m_{gas} - m_{gpdr}}{m_{gas}} \tag{2}$$

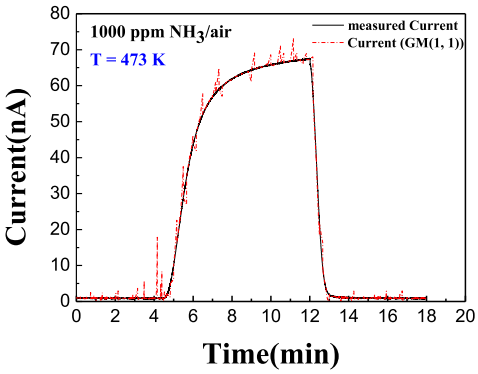

FIGURE 9. **Comparison of measured raw sensing data and recovery sensing data by using GM(1, 1) under 1000 ppm NH_3/air gas at 473K.**

where n is the number of data sets, and m_{gas} and m_{gpdr} are the data for the ammonia sensing and GPDR model output. In this case, MRE (%) is only 56.85%. This value needs to be improved; the dissatisfaction is mainly caused by the first-order differential fitting. Our GPDR model can overcome this problem. The simulation steps are as follows.

Step 1: Take three sets of data from the ammonia sensing response starting point (D(k), $1 \le k \le 3$), and then 1-AGO, $D^{(1)}$ can be obtained:

$$D^{(1)} = \left\{ \sum_{i=1}^{k} D(i), 1 \le k \le 3 \right\}. \tag{3}$$

Step 2: Set $D^{(1)}$ with a one-dimensional polynomial type:

$$D^{(1)}(k) = ak^2 + bk + c, for 1 \le k \le 3. \tag{4}$$

Step 3: Take $1 \le k \le 3$ from Step 2, so that the coefficient value can be obtained.

$$\begin{bmatrix} a \\ b \\ c \end{bmatrix} = \begin{bmatrix} D^{(1)}(1) \\ D^{(1)}(2) \\ D^{(1)}(3) \end{bmatrix} \begin{bmatrix} 1 & 1 & 1 \\ 4 & 2 & 1 \\ 9 & 3 & 1 \end{bmatrix}^{-1}. \tag{5}$$

Step 4: Find the estimated value $\widehat{D}(k+1)$:

$$\widehat{D}(k+1) = \widehat{D}^{(1)}(k+1) - \widehat{D}^{(1)}(k). \tag{6}$$

Step 5: Find the differences between the original results and GPDM data.

Step 6: Replace these simulation data from step 5 with the actual sensing data.

Step 7: Add three consecutive measured points based on step 6, interval every 100 points.

By performing steps 1 through 7, the redundant data will be removed. The remaining data can be transferred to the server for storage and analysis. The reduced data received by the server can be processed according to steps 1 through 4 to obtain the simulated recovery value. Figure 10 shows the

corresponding simulated results from the GPDR model. The MRE (%) is 96.76%, which is higher than that of GM(1, 1). Table 1 shows the reduction point ratio and recovery rate of the GPDR model at different intervals. At 50 point intervals, 1000 ppm NN3/air was introduced at an operating temperature of 423 K; the ratio of reduction points is 64.22%, and the recovery rate can be as high as 99.79%.

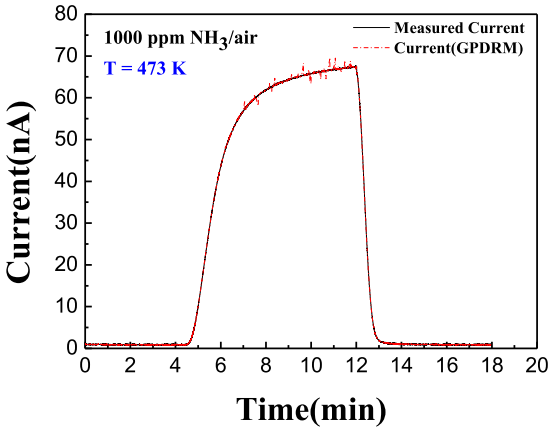

FIGURE 10. **Comparison of measured raw sensing data and recovery sensing data by using GPDR model under 1000 ppm NH_3/air gas at 473K.**

TABLE 1. **Comparison of reduced data rate and recovery rate with different interval points by using GPDR model.**

Interval points	Reduced Number Rate (%)	Recovery error rate (%)
50	64.22	0.21
100	71.84	3.24
200	80.07	20.65
500	82.01	26.37

V. CONCLUSION

In summary, a new Pt/NiO/GaN-based MOS diode-type ammonia sensor was fabricated. The related ammonia sensing performance was studied and reported. Although a relatively higher operating temperature (≥423 K) was needed, the studied device shows good ammonia sensing properties. Experimentally, a high sensing response of 244.2 was obtained under the introduced 1000 ppm NH_3/air gas at 423 K. This value is remarkably higher than those reported by Schottky diode-type ammonia sensors. Even under a lower ammonia concentration of 2 ppm NH_3/air, the studied device presents distinct sensing behaviors. The studied device also provides advantages of operating flexibility in both applied forward and reverse voltages and reversible sensing performance. In addition, we developed a new GPDR model to reduce the redundant data and achieve a high recovery rate. This is promising for the transmission of sensing data in IoT applications.

ACKNOWLEDGMENT

The authors would like to acknowledge Miss Hui-Jung Shih for her excellent technical support at Instrument Center, National Cheng-Kung University.

REFERENCES

[1] H.-W. Zan, W.-W. Tsai, Y.-R. Lo, Y.-M. Wu, and Y.-S. Yang, "Pentacene-based organic thin film transistors for ammonia sensing," *IEEE Sensors J.*, vol. 12, no. 3, pp. 594–601, Mar. 2012.

[2] S. G. Pawar *et al.*, "Room temperature ammonia gas sensor based on polyaniline-TiO_2 nanocomposite," *IEEE Sensors J.*, vol. 11, no. 12, pp. 3417–3423, Dec. 2011.

[3] H. M. ApSimon, B. M. Barker, and S. Kayin, "Modeling studies of the atmospheric release and transport of ammonia in anticyclonic episodes," *Atmos. Environ.*, vol. 21, no. 4, pp. 1939–1946, 1967.

[4] S. Yamulki, R. M. Harrison, and K. W. T. Goulding, "Ammonia surface-exchange above an agricultural field in Southeast England," *Atmos. Environ.*, vol. 30, no. 1, pp. 109–118, 1996.

[5] R. L. Knight, R. H. Kadlec, and H. M. Ohlendorf, "The use of treatment wetlands for petroleum industry effluents," *Environ. Sci. Technol.*, vol. 33, no. 7, pp. 973–980, 1999.

[6] Yewale, K. Raulkar, A. Wadatkar, and G. Lamdhade, "Application of metal oxide thick film as a NH_3 gas sensor," *J. Electron Devices*, vol. 11, pp. 544–550, Apr. 2011.

[7] A. J. Kulandaisamy *et al.*, "Room temperature ammonia sensing properties of ZnO thin films grown by spray pyrolysis: Effect of Mg doping," *J. Alloys Compounds*, vol. 688, pp. 422–429, Dec. 2016.

[8] N. D. Dien, D. D. Vuong, and N. D. Chien, "Hydrothermal synthesis and NH_3 gas sensing property of WO_3 nanorods at low temperature," *Adv. Nat. Sci. Nanosci. Nanotechnol.*, vol. 6, no. 3, 2015, Art. no. 035006.

[9] R. K. Gangopadhyay and S. K. Das, "Ammonia leakage from refrigeration plant and the management practice," *Process Safety Progress*, vol. 27, no. 1, pp. 15–20, 2008.

[10] M. J. Fedoruk, R. Bronstein, and B. D. Kerger, "Ammonia exposure and hazard assessment for selected household cleaning product uses," *J. Expo. Anal. Environ. Epidemiol.*, vol. 15, no. 6, pp. 534–544, 2005.

[11] V. B. Raj *et al.*, "Cross-sensitivity and selectivity studies on ZnO surface acoustic wave ammonia sensor," *Sensors Actuators B Chem.*, vol. 147, no. 2, pp. 517–524, 2010.

[12] S.-K. Lee, D. Chang, and S.W. Kim, "Gas sensors based on carbon nanoflake/tin oxide composites for ammonia detection," *J. Hazard Mater.*, vol. 268, pp. 110–114, Mar. 2014.

[13] V. Talwar, O. Singh, and R. C. Singh, "ZnO assisted polyaniline nanofibers and its application as ammonia gas sensor," *Sensors Actuators B Chem.*, vol. 191, pp. 276–282, Feb. 2014.

[14] G. Wang *et al.*, "Fabrication and characterization of polycrystalline WO_3 nanofibers and their application for ammonia sensing," *J. Phys. Chem. B*, vol. 110, no. 47, pp. 23777–23782, 2006.

[15] C.-S. Hsu *et al.*, "Ammonia gas sensing performance of an indium tin oxide (ITO) based device with an underlying Au-nanodot layer," *J. Electrochem. Soc.*, vol. 160, no. 2, pp. B17–B22, 2013.

[16] P.-C. Chou *et al.*, "On the ammonia gas sensing performance of a RF sputtered NiO thin-film sensor," *IEEE Sensors J.*, vol. 15, no. 7, pp. 3711–3715, Jul. 2015.

[17] H.-I. Chen *et al.*, "Characteristics of a Pt/NiO thin film-based ammonia gas sensor," *Sensors Actuators B Chem.*, vol. 256, pp. 962–967, Mar. 2018.

[18] S. W. Jung, K. H. Baik, F. Ren, S. J. Pearton, and S. W. Jang, "AlGaN/GaN heterostructure based Schottky diode sensors with ZnO nanorods for environmental ammonia monitoring applications," *ECS J. Solid State Sci. Technol.*, vol. 7, no. 7, pp. Q3020–Q3024, 2018.

[19] T.-Y. Chen *et al.*, "Ammonia sensing characteristics of a Pt/AlGaN/GaN Schottky diode," *Sensors Actuators B Chem.*, vol. 155, no. 1, pp. 347–350, 2011.

[20] P.-C. Chou *et al.*, "Study of an electroless plating (EP)-based Pt/AlGaN/GaN Schottky diode-type ammonia sensor," *Sensors Actuators B Chem.*, vol. 203, pp. 258–262, Nov. 2014.

[21] S. C. Hung, W. Y. Woon, S. M. Lan, F. Ren, and S. J. Pearton, "Characteristics of carbon monoxide sensors made by polar and nonpolar zinc oxide nanowires gated AlGaN/GaN high electron mobility transistor," *Appl. Phys. Lett.*, vol. 103, no. 8, 2013, Art. no. 083506.

[22] C.-F. Lo *et al.*, "Effect of temperature on CO sensing response in air ambient by using ZnO nanorod-gated AlGaN/GaN high electron mobility transistors," *Sensors Actuators B Chem.*, vol. 176, pp. 708–712, Jan. 2013.
[23] J.-H. Suh *et al.*, "Fully integrated and portable semiconductor-type multi-gas sensing module for IoT applications," *Sensors Actuators B Chem.*, vol. 265, pp. 660–667, Jul. 2018.
[24] O. Blanco-Novoa, T. M. Fernández-Caramés, P. Fraga-Lamas, and L. Castedo, "A cost-effective IoT system for monitoring indoor radon gas concentration," *Sensors*, vol. 18, no. 7, 2018, Art. no. E2198.
[25] D. Struk, A. Shirke, A. Mahdavifar, P. J. Hesketh, and J. R. Stetter "Investigating time-resolved response of micro thermal conductivity sensor under various modes of operation," *Sensors Actuators B Chem.*, vol. 254, pp. 771–777, Jan. 2018.
[26] D. Ju-Long, "Control problems of grey systems," *Syst. Control Lett.*, vol. 1, no. 5, pp. 288–294, 1982.
[27] H. Hsieh, H. C. Chen, and R. H. Huang, "Gray polynomial model," *J. Gray Syst.*, vol. 19, no. 3, pp. 203–208, Sep. 2007.
[28] K.-W. Lin and C.-S. Hsu, "Analysis of hydrogen gas sensing characteristics based on a grey polynomial differential model (GPDM) algorithm," *IEEE Sensors J.*, vol. 11, no. 9, pp. 1894–1898, Sep. 2011.
[29] K.-W. Lin *et al.*, "Characteristics of a new Pt/oxide/$In_{0.49}Ga_{0.51}P$ hydrogen-sensing Schottky diode," *Sensors Actuators B Chem.*, vol. 94, no. 2, pp. 145–151, 2003.
[30] J.-R. Huang *et al.*, "Investigation of hydrogen-sensing characteristics of a Pd/GaN Shottky diode," *IEEE Sensors J.*, vol. 11, no. 5, pp. 1194–1200, May 2011.
[31] C.-Y. Chi, H.-I. Chen, W.-C. Chen, C.-H. Chang, and W.-C. Liu, "Formaldehyde sensing characteristics of an aluminum-doped zinc oxide (AZO) thin-film-based sensor," *Sensors Actuators B Chem.*, vol. 255, pp. 3017–3024, Feb. 2018.
[32] T.-Y. Chen *et al.*, "Characteristics of ZnO nanorods-based ammonia gas sensors with a cross-linked configuration," *Sensors Actuators B Chem.*, vol. 221, pp. 491–498, Dec. 2015.
[33] H.-I. Chen *et al.*, "Ammonia sensing characteristic of a Pt nanoparticle/aluminum-doped zinc oxide sensor," *Sensors Actuators B Chem.*, vol. 267, pp. 145–154, Aug. 2018.
[34] D. Wang, S. F. Yin, C. Chen, J. H. Wu, and G. L. Wang, "Application of GM(1,1) model on predicating the outpatient amount," *Adv. Multimedia Softw. Eng. Comput.*, vol. 2, pp. 71–76, 2011.
[35] C. F. Lucchinetti *et al.*, "A role for humoral mechanisms in the pathogenesis of Devic's neuromyelitis optica," *Brain*, vol. 125, pp. 1450–1461, Jul. 2002.

I-PING LIU received the B.S., M.S., and Ph.D. degrees from the Department of Chemical Engineering, National Cheng Kung University, Tainan, Taiwan, in 2007, 2011, and 2017, respectively. His research has focused on quantum dot-based solar cells and semiconductor gas sensors.

CHING-HONG CHANG was born in Taipei, Taiwan, in 1991. He is currently pursuing the Ph.D. degree with the Institute of Microelectronics, National Cheng Kung University, Tainan, Taiwan. His research has focused on semiconductor sensors and MOS-field electron transistor and E-mode HEMT.

YEN-MING HUANG received the M.S. degree from National Cheng Kung University, Tainan, Taiwan, in 2018. His research has focused on MOS-field electron transistor and E-mode HEMT.

KUN-WEI LIN received the B.S. degree from the Department of Electric Engineering, Fu Jen Catholic University, New Taipei City, Taiwan, in 1995, and the M.S. and Ph.D. degrees from the Department of Electric Engineering, National Cheng Kung University, Tainan, Taiwan, in 1997 and 2003, respectively. He is currently an Associate Professor with the Department of Computer Science and Information Engineering, Chaoyang University of Technology, where he was the Department Chair of computer science and information engineering from 2009 to 2012. His current research focuses on gas sensors, circuit design, data analysis, and Internet of Things.